ÆGIS

An Astrophysics Experiment for Grating and Imaging Spectroscopy

A high-throughput, high-resolution, moderate cost, soft X-ray spectrometer

A mission concept to be presented to NASA in response to the Request for Information on
"Concepts for the Next NASA X-ray Astronomy Mission"
(Solicitation Number NNH11ZDA018L)

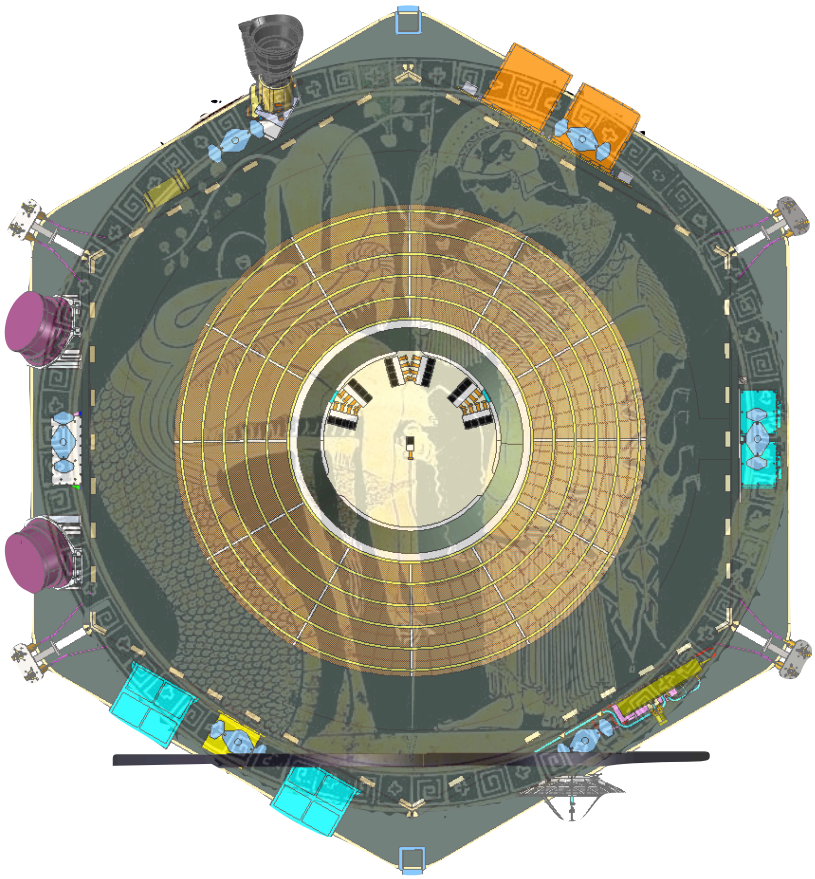

M. W. Bautz (mwb@space.mit.edu, 617-253-7502)
Senior Research Scientist & Associate Director
Kavli Institute for Astrophysics and Space Research
Massachusetts Institute of Technology

G. E. Allen	J. Bookbinder	D. Bower	J. Bregman	N. Brickhouse
D. N. Burrows	C. R. Canizares	S. Casement	D. Chakrabarty	K.-W. Chan
B. Costello	J. E. Davis	D. Dewey	J. J. Drake	M. S. Elvis
D. Evans	A. Falcone	K. Flanagan	R. K. Heilmann	J. C. Houck
D. P. Huenemoerder	S. Jordan	A. Klavins	J. C. Lee	J. Lempke
C. Lillie	M. Loewenstein	H. L. Marshall	S. Mathur	R. S. McClelland
J. M. Miller	R. Mushotzky	T. Nguyen	F. Nicastro	M. A. Nowak
S. L. O'Dell	F. Paerels	R. Petre	A. Ptak	T. T. Saha
M. L. Schattenburg	N. Schulz	R. K. Smith	D. Tenerelli	R. Vanbezooijen
G. Vasudevan	D. Wang	S. Wolk	W. W. Zhang	

28 October 2011

1 Summary

A compelling portion of the science achievable by the International X-ray Observatory (IXO), as judged by the Astro2010 Decadal Survey, was made possible by IXO's X-ray Grating Spectrometer (XGS). With an effective area exceeding 1000 cm^2 and a spectral resolving power $R = \lambda/\Delta\lambda > 3000$, the IXO XGS was designed to address a broad range of fundamental questions, including *"How does cosmic feedback connect the growth of supermassive black holes with that of large-scale structure?"; "How does large scale structure evolve?"; "What happens close to a black hole?";* and *"How does matter behave at very high density?"* The IXO XGS offered more than an order-of-magnitude increase in effective area over current X-ray spectrometers, and unprecedented spectral resolution. Had IXO been developed, its XGS would undoubtedly have driven enormous progress on these questions and on many others as well.

Here we respond to NASA's Request for Information on Concepts for the Next NASA X-ray Astronomy Mission (RFI) by describing ÆGIS, an Astrophysics Experiment for Grating and Imaging Spectroscopy. At a small fraction of the cost of IXO, ÆGIS provides capabilities that surpass IXO XGS requirements, and are far superior to those of any existing soft X-ray spectrometer. Just one of the many dramatic advances ÆGIS enables is illustrated in Figure 1, which compares the capability of ÆGIS to measure line centroids, and thus line-of-sight velocities, to that of previous instruments. At the crucial K lines of OVII and OVIII, for example, ÆGIS's statistical precision is 40 times better than that of any previous spectrometer. Moreover, no planned micro-calorimeter is competitive with ÆGIS in its 0.2 - 1 keV band, where many of the most astrophysically important lines are located. As we discuss in detail below, ÆGIS provides comparable breakthroughs in line-detection and equivalent-width measurement capability.

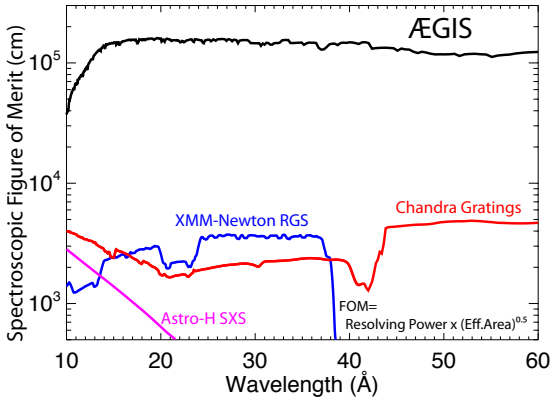

Figure 1: *ÆGIS is 30 - 50 times more sensitive than any existing soft X-ray spectrometer, and will bring the power of X-ray line spectroscopy to a vast range of objects and phenomena beyond the reach of current instruments. The figure of merit indicates accuracy of line centroid (and thus velocity) measurement.*

High-resolution line spectroscopy has provided much of our astrophysical knowledge. ÆGIS will make this technique as powerful in X-ray astronomy as it has become in other wavebands. Atomic physics renders almost all of the ionization states of all of the abundant elements accessible in its passband, so ÆGIS can provide a comprehensive physical picture often unavailable in other wavebands, where diagnostics from only a small number of ionization states and/or elements exist. At the same time, ÆGIS will enable powerful multi-wavelength investigations, for example with Hubble/COS in the UV to characterize the intergalactic medium. ÆGIS will be the first observatory with sufficient resolution at $E < 1$ keV to resolve thermally-broadened lines in hot ($T \gtrsim 10^7$ K) plasmas, and with its superb sensitivity it will do so in a broad range of objects. This sensitivity will also undoubtedly produce unanticipated new discoveries, as profound, perhaps, as the finding by the grating spectrometers on XMM and Chandra that something must be heating cool galaxy cluster cores. The search for that heat source has revolutionized our understanding of cosmic feedback.

ÆGIS incorporates innovative technology in X-ray optics, diffraction gratings and detectors. The flight mirror uses the high area-to-mass ratio segmented glass architecture developed for IXO, but with smaller aperture and with larger graze angles optimized for high-throughput grating spectroscopy at minimum mass and cost. The unique Critical Angle Transmission (CAT) gratings, also considered for IXO, combine the low mass and relaxed figure and alignment tolerances of the transmission gratings on Chandra with the high diffraction efficiency and resolving power of blazed reflection gratings. For maximum spectral resolution, each of six parallel CAT grating spectrometers is illuminated by a sub-aperture of the flight mirror. Technology development is advancing successfully in accordance with detailed development plans, consisent with an ÆGIS new start at the midpoint of the current decade.

As befits the broad range of astrophysics it will address, ÆGIS will be available to the entire astronomical community. A cost-effective Falcon-9 launcher is baselined to bring the observatory to its L2 orbit, where observing efficiency is maximized. In the baseline three-year mission ÆGIS will record more than four times as much on-source exposure as was planned for the IXO XGS, with greater sensitivity. Using an efficient operations model, and with a substantial general observer program, the ÆGIS ROM mission cost, at $\sim$ \$758M (FY2012), lies near the low end of the RFI's medium cost category.

Among national space agencies engaged in high-energy astrophysics, only NASA is prepared to furnish the high-resolution grating spectroscopy capability X-ray astronomy must have. ESA's ATHENA mission, in particular, would have no grating spectrometer. Here we show that NASA can provide this crucial capability at moderate cost by developing ÆGIS.

2 ÆGIS Science

ÆGIS outperforms current X-ray grating spectrometers on Chandra and XMM by more than an order of magnitude, as we show in Figure 2. It took 10 days to get a single high quality Chandra HETGS spectrum of a bright Active Galactic Nucleus (AGN). ÆGIS will do as well in just 4 hours, about the light crossing time for a 10^8 $M_\odot$ black hole, making spectra of such quality routine. The superb resolving power will allow detailed kinematic studies of galactic outflows, hot gas in galactic halos, and stellar accretion. ÆGIS will address many fundamental astrophysical problems highlighted in the 2010 Decadal Survey "New Worlds, New Horizons in Astronomy and Astrophysics,"[11] NWNH, and especially those to be addressed by IXO[3,4] as listed in Table 1.

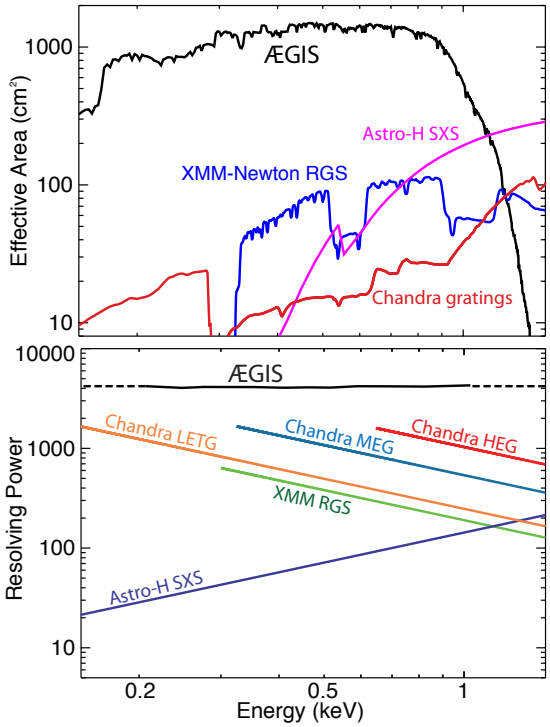

Figure 2: *ÆGIS has a greater effective area (top) and higher resolving power (bottom) than any other instrument. ÆGIS' values are based on end-to-end Monte-Carlo ray-trace simulations.*

ÆGIS X-ray absorption-line spectroscopy of objects throughout the Universe will advance our knowledge of large scale structure, cosmic feedback, and the growth of black holes. Chandra and XMM have been used on the few brightest sources in the sky to study the interstellar medium (ISM). ÆGIS can observe *thousands* of cosmic X-ray sources to systematically study neutral and ionized matter to great distances. These investigations will reveal the composition, distribution, and kinematics of matter in the Galaxy, the local Universe, and beyond.

ÆGIS will reveal the physics that drives disk accretion, and its radiative and mechanical feedback for both supermassive and stellar-mass black holes as well as other compact objects. Spectra of large samples of pre-main sequence stars will show how the accretion process creates stars, studies that can only be done on a few sources today. Observations of main sequence stars will resolve many puzzles concerning the interplay of rotation, magnetic fields and stellar type in generating coronal emission, and at the same time address questions involving X-ray effects on planets throughout their lifetimes.

In Table 1, we map IXO science questions to ÆGIS

Science Questions	Measurements	Performance Requirements
IXO Science		
What is the relation between SMBH formation & evolution of Large Scale Structure? ("cosmic feedback") (§§2.1.1, 2.1.2)	Line absorption positions, strengths, profiles in AGN; resolve flow velocities.	$R \geq 3000$; $A_{\rm eff} \geq 1000\,{\rm cm}^2$ $\Delta v \geq 100\,{\rm km\,s}^{-1}$ Bandpass: 0.2–1.0 keV; $\Delta\theta \leq 10$ arcsec
How does Large Scale Structure evolve? (§§2.1.1, 2.1.2)	Measure WHIM absorption (in C, N, O) against background AGN; measure mass and composition of galaxy clusters at redshifts < 2.	Equivalent width: $W_\lambda = 2\,{\rm m\AA}$ Bandpass: 0.2–1.0 keV $R \geq 3000$ $A_{\rm eff} \geq 1000\,{\rm cm}^2$
What happens close to a black hole? (§2.2.2)	Line absorption & variability in XRB soft state.	$R \geq 3000$; $A_{\rm eff} \geq 1000\,{\rm cm}^2$ Timing; $f \leq 15$ Hz;
How does matter behave at very high density? (§2.2.2)	Search for lines in long outbursts of slowly rotating NS.	$R \geq 3000$; $A_{\rm eff} \geq 1000\,{\rm cm}^2$ Timing; $f \leq 15$ Hz; Bandpass: 0.2–1.0 keV
Additional NWNH Science		
How rapidly did high-energy radiation of young stars disperse their disks? (§2.3)	Emission line flux, velocity, width of C, N, O, Ne, Fe; flux & velocity variability;	$v \leq 20\,{\rm km\,s}^{-1}$, $\Delta v \leq 100\,{\rm km\,s}^{-1}$, Bandpass: 0.2–1.0 keV, $A_{\rm eff} \geq 1000\,{\rm cm}^2$, $\Delta t \sim 0.2$ day
How do rotation & magnetic fields affect stars? (§2.3)	Emission line flux, velocity, width of C, N, O, Ne, Fe; flux & velocity variability; resolve thermal width at 10^7 K	$v \leq 20\,{\rm km\,s}^{-1}$, $\Delta v \leq 100\,{\rm km\,s}^{-1}$, Bandpass: 0.2–1.0 keV, $\Delta t \geq 200$ s (flares)

Table 1: *ÆGIS scientific questions, measurements and performance requirements. References to pertinent sections of this paper are given in the first column.*

measurements and requirements. We also list other high priorities of NWNH that ÆGIS will address.

2.1 Matter in and between Galaxies

2.1.1 Galactic Structure and Feedback

What are the detailed abundances, kinematics, and morphologies of the cold, warm, and hot phases of the ISM in our Galaxy? What is the composition and state of matter in other galaxies and in the IGM? ÆGIS can address these issues of cosmic feedback affecting the growth of large scale structure and interactions with supermassive black holes (SMBH).

The soft X-ray band is sensitive to K-shell absorption from the high abundance elements C, N, O, Ne as well as L-shell absorption by Si, S, Ca, and Fe. ÆGIS will measure these elements in all phases and forms in the local universe. Detection of several transitions in one or more ions of different elements lets us fully determine thermal state, turbulent width, ionization balance, and abundances. This capability is not limited to gas-phase material. Cold ISM phases also have dust signatures in this X-ray band directly measurable[34] through near-edge absorption and scattering.

Metals in the Milky Way: The high ÆGIS throughput and spectral resolution will allow us to improve upon Chandra by determining to high precision the *quantity and composition* of gas and dust on an element-by-element basis, as well as their charge states[33,35] (see Figure 3). This is not possible in any other waveband. Such precision measurements of the composition, distribution, and depletion levels in space environments (local and extragalactic) are crucial for improving our understanding of a wide range of astrophysical processes from nucleosynthesis to planet formation, with potential additional consequences for cosmology[49].

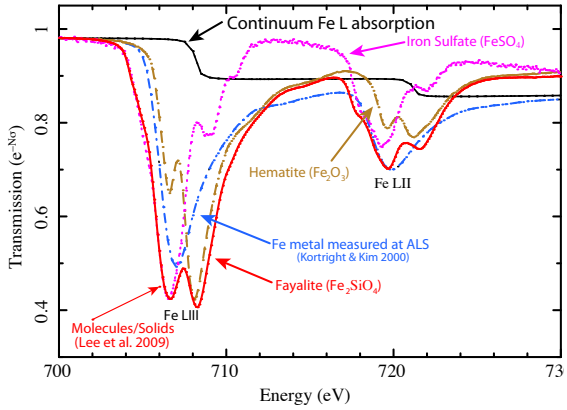

Figure 3: *ÆGIS can determine the molecular Fe content and distribution of interstellar dust. and measure the metallic Fe L-edge (from Lee et al.[34])*

ÆGIS absorption line studies of C, N, O, and Ne features will map the structure of the the ISM and hot halo of the Milky Way. From the few objects bright enough for such studies with Chandra and XMM, we know that these lines are strong diagnostics of the states of neutral and ionized matter. ÆGIS can observe about 5000 Galactic sources ($f_x > 10^{-13}$ to $10^{-9}\,\mathrm{ergs\,cm^{-2}\,s^{-1}}$) for Milky Way ISM and halo studies.

Metals in Other Galaxies: Accurate determinations of abundances, structure, and kinematic properties of the ISM and halos of other galaxies (including the LMC, SMC, and M31) will greatly improve our understanding of galactic interfaces with the IGM and the importance of cosmic feedback. ÆGIS can easily observe a number of bright ($f_x \sim 10^{-12}\,\mathrm{ergs\,cm^{-2}\,s^{-1}}$) sources in M31 with $\sim 10\,\mathrm{ks}$ exposures. In the local universe there are at least 150 nearby galaxies with sufficient flux ($f_x > 10^{-13}\,\mathrm{ergs\,cm^{-2}\,s^{-1}}$) for ÆGIS spectroscopy. XMM data have revealed a new and potentially powerful diagnostic of hot-cold gas interfaces in other galaxies: unusual line ratios in He-like ions suggest that charge exchange is an important process.[37,38] Confirmation by ÆGIS would show that interactions between hot and cool gas are common, with strong implications for ISM modeling.

While designed for point sources, the ÆGIS spectrometer will retain $R \geq 300$ for sources up to $\sim 30\,\mathrm{arcsec}$ in size, adequate to resolve cluster cores and the inner, high surface brightness, portions of elliptical galaxies. By providing an order of magnitude more resolving power than Astro-H for C and N emission lines, ÆGIS can reliably constrain the abundances of these elements that are produced via nucleosynthetic channels distinct from higher-Z elements. Extending the measured abundance pattern to C and N places strong new constraints on the star formation history and initial mass function in these systems. XMM RGS observations of elliptical galaxies have shown subsolar Fe, O, and Ne abundances, while the available data suggests N is solar or even supersolar.[56] The subsolar results conflict with theoretical models based on optical measurements of stellar metallicities and SNIa rates in ellipticals, implying the need for a fundamental re-evaluation of elliptical galaxy metal enrichment.[39,50] Since C and N are hydrostatically produced with distinctive yield dependencies on progenitor mass and expelled in stellar winds, while other elements arise explosively from supernovae, measurements of these lines are key to distinguishing models for the origin of metals in ellipticals and the timescale of their injection. ÆGIS observations of ellipticals in a range of environments will resolve this issue.

Missing Baryons in Galaxies: Optical observations have shown that most galaxies are missing more than $2/3$ of their baryons, relative to their cosmological ratio with dark matter.[29] Non-detections in IR, optical, and UV bands suggest that these missing baryons are hot, but we do not know if they are present in the Galactic halo or in the Local Group,[6] either as expelled in a Galactic wind or preheated so that they simply never coalesced during the formation of the Galaxy.[46,57]

A diagnostic for distinguishing between Galactic and Local Group components is the velocity of the gas, which should vary by $\sim 100\,\mathrm{km\,s^{-1}}$.[47] The difference between the heliocentric velocity and the Galactocentric velocity can be up to $\sim 200\,\mathrm{km\,s^{-1}}$, while M31 and the Local Group differ by $\sim 300\,\mathrm{km\,s^{-1}}$. ÆGIS can thus distinguish a hot Galactic halo rotating with the Milky Way from the Local Group IGM by measuring velocity as a function of longitude.

2.1.2 Intergalactic Medium

As less than 10% of the baryons in the local Universe lie in galaxies as stars or cold gas[19], the remainder are predicted to exist as a dilute gaseous filamentary network – the *cosmic web*.[10] Half of this cosmic web is detected in narrow Lyα ($\sim$ 30%) or O VI ($\sim$ 10%)[13], and in broad Lyα absorption lines ($\sim$ 10%)[14], but half remains undetected despite vigorous searches. Growth-of-structure simulations predict that these "missing" baryons are shock-heated up to temperatures of 10^{6-7} K in unvirialized cosmic filaments and may (or may not) be chemically enriched by galactic superwinds – the Warm-Hot Intergalactic Medium (WHIM; see Figure 4). This distribution of mass as a function of temperature can be determined from X-ray absorption line spectroscopy of highly ionized C, N, O, and Ne detected against background AGNs. Surprisingly, even stacked searches of sightlines that show O VI in absorption do not reveal X-ray absorption lines,[58] suggesting that either the filaments seen by the HST COS are a distinct warm population separate from the hot fraction, or that our models of structure formation and enrichment must be revised. ÆGIS can detect far smaller filaments than any current or planned instrument (see Figure 5). Based on the Cen & Fang[9] model and using sources selected from the ROSAT blazar catalog[55], we expect to detect $\sim$ 100 systems with both O VII and O VIII features with equivalent widths ranging from 2–5 mÅ.[5] Furthermore, the high ÆGIS resolving power will allow us to discriminate thermal from Hubble-flow, and to resolve internal turbulence widths in ions such as C and Ne, effects which determine line depths and are crucial to derivation of elemental abundances.

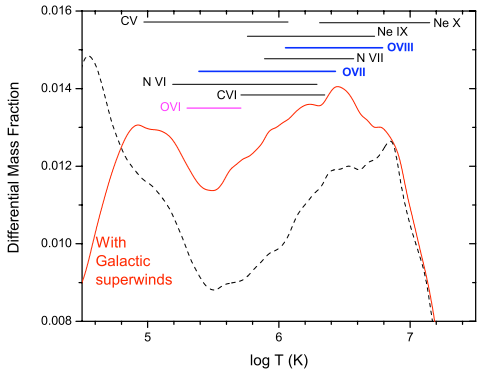

Figure 4: *ÆGIS will distinguish between two possible models of IGM enrichment, those with superwinds (solid red curve), or those without (dashed black curve). Horizontal bars show the temperature ranges of emission for different ions whose resonance lines (except for O VI) are in the 0.2 – 1.0 keV band. (from Cen & Ostriker[10])*

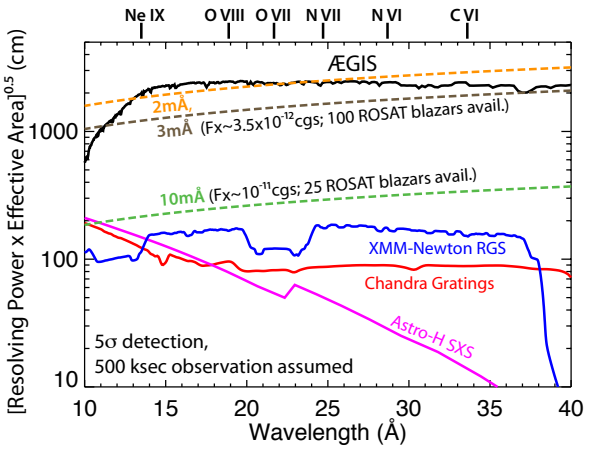

Figure 5: *ÆGIS has a line detection sensitivity which is an order of magnitude better than any other instrument.*

As the baryons are yet unseen, the optimum distribution of sight lines and exposure times cannot be predetermined. ÆGIS can detect filaments with O abundance as low as 0.03 of solar in $\sim$ 500 ks. These observations will also reveal the role of galactic superwinds in enriching the web both from the proximity of the absorbers to galaxies and from the kinematics of the hot gas (see Figure 6 and Section 2.1.1).

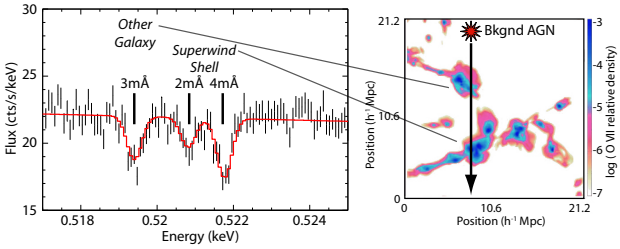

Figure 6: *ÆGIS can detect WHIM absorption at theoretically expected levels. These 3 differently-redshifted components of the WHIM in O VII Kα are near minimum detectability. The left panel shows the spectrum, and the right indicates the geometry, with a bright background source (top) shining through filaments to an observer at the bottom.*

2.2 Matter in and around Compact Objects

2.2.1 Active Galactic Nuclei

NWNH identified two related key questions: *"What are the flows of matter and energy in the circumgalactic medium?"* and *"How do black holes grow, radiate, and influence their surroundings?"*, tied together by a common theme of feedback.

At pc scales, there is a competition between the fueling of the hole and outflowing winds, seen as "warm absorbers" commonly found in the soft X-ray spectra of AGN.[51] The HETGS and RGS are now used to measure ionization parameters, columns, and velocities of this gas.[30] Mass outflow rates may exceed the mass accretion rate onto the hole[2] but the mass and energy outflow rates depend critically on the distances of the wind origins from their ionizing sources and on wind densities, which are poorly known. Ionization variability studies have yielded density estimates for the brightest sources[32,45,52] and ÆGIS observations will extend this technique to shorter time scales (for gas closest to the cores) and fainter AGN such as radio loud galaxies that appear to heat intracluster gas. Furthermore, the ÆGIS spectral resolution is needed to clarify the connection between the UV and X-ray absorbing gas; some X-ray features match two or more UV/optical components, while other absorption lines have no counterparts.[12] Another technique to measure densities could be pioneered with ÆGIS due to its improved sensitivity. Ratios of metastable lines such as those of Si X, and S XII (near 50.7 Å and 36.5 Å) to the corresponding ground states would give density estimates in the 10^{6-11} cm^{-3} range.[36]

At kpc scales, active nuclei ionize outflowing gas. HETGS observations of the canonical Seyfert 2 galaxy NGC 1068 clearly reveal separate components: blue-shifted and Doppler broadened emission associated with the nucleus, and red-shifted emission associated with an *outflowing* photo-ionized gas[16] (see Figure 7). The role of such outflows in galaxy feedback processes is still an issue of debate.[32] The large effective area of ÆGIS will extend these studies to fainter off-axis outflows. Furthermore, in a single observation ÆGIS will provide six different observing angles, which will allow for spatial-spectral modeling of AGN nuclei and ionization cones.

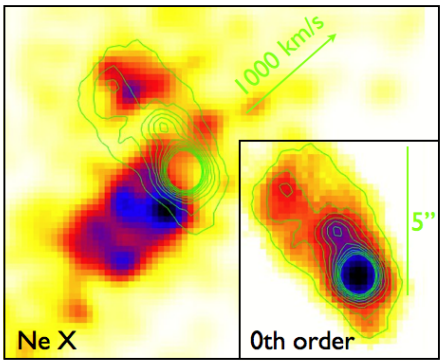

Figure 7: *ÆGIS will provide spatially resolved spectra of AGN, as in this HETGS "Doppler image" of Ne X emission in NGC 1068; overlain by contours from the 0th order image (inset) at the systemic velocity. Ne X; the arrow shows a* $1000\,\mathrm{km\,s^{-1}}$ *redshift along the HETGS dispersion direction. The AGN central source emission is blue-shifted by -700* $\mathrm{km\,s^{-1}}$*, while off-nuclear photoionized gas to the NE of the core is offset +150* $\mathrm{km\,s^{-1}}$.

ÆGIS may even be able to test physics in strong gravity. Three AGN show evidence of relativistically broadened Fe-L emission lines arising from the inner accretion disk[18,44,48], although the spectra may be complicated by line blends from ionized absorbers along the line of sight. If present, ÆGIS will easily resolve broad features from any interloping narrow lines, and potentially could time-resolve emission from hot spots on the disk, testing General Relativity as proposed using Fe-K lines[54]. Interpretations are still controversial, but the scientific potential is great.

2.2.2 Galactic Compact Objects

Galactic black holes also can exhibit rich line spectra that probe their local environment and also provide evidence of feedback in their accretion processes. HETGS observations show that high mass X-ray binary systems such as Cyg X-1 are fed by "focused accretion winds" exhibiting a wide range of ionization parameters and densities[24]. *Variations in the properties of the focused wind occur faster than can be studied with the small effective areas of Chandra-HETG and XMM-RGS.* Transient low mass X-ray binary systems show a fascinating evolution of accretion properties as they move from a corona- and jet-dominated "hard state" to a wind- and disk-dominated spectrally "soft state"[42,43]. GRO J1655−40 first exhibits Fe XXV and Fe XXVI absorption as it begins the transition out of a jet-dominated state, which evolves into *extremely strong, lower ionization* absorption as it fully enters a state dominated by a disk and wind, which is best diagnosed in the $0.2\text{-}1\,\mathrm{keV}$ band. Models indicate that the wind is *not* driven by radiation, but rather must be driven by magnetic processes in the disk. Observations of such systems have been rare, and the transition from jet, to wind, to "quiet" (albeit bright) accretion disk is not yet understood.

Neutron stars also have exhibited a rich variety of absorption features; however, most have been associated with absorption in the outer disk in near edge-on systems. One exception has been IGR J17480−2446, a neutron star binary in the Terzan 5 globular cluster. HETGS observations have shown Fe XXV and Fe XXVI absorption consistent with a radiatively driven wind[41]. More interestingly, this NS has only an $11\,\mathrm{Hz}$ spin period, meaning that it is a strong candidate for spectroscopic searches for atmospheric lines in the NS atmosphere, which are otherwise expected to be smeared out in rapidly rotating systems. This source was a transient, but it does demonstrate that a population of slowly rotating NS exists. Detection of photospheric absorption lines and edges will allow a direct, distance- and luminosity-independent measurement of mass and radius, through measurement of the gravitational redshift and the effect of pressure broadening on line equivalent widths and blurring of photoionization edges. The prime spectral series for these diagnostics are the Balmer and Paschen series or their analogs, in Fe XXV and Fe XXVI, in the 7-13 and 16-36 Å bands (assuming a gravitational redshift of 0.3).

2.3 From Disks to Stars and Planets

A priority of NWNH is the understanding the effect of high-energy radiation on protoplanetary disks (see Table 1). X-rays can strongly affect the dynamical structure of a protoplanetary accretion disk.[20] Coupling between the disk and stellar coronal magnetic fields can funnel accretion streams leading to shocks, and can also generate energetic, hard X-ray flares from reconnection of large magnetic loops. Whether disk evolution leads to planet formation depends on the detailed influence of ionizing radiation on the disk.[1] Even after an accretion disk dissipates, stellar coronal X-rays can be powerful enough to alter or even erode atmospheres of close-in planets.[53] High-resolution X-ray spectroscopy can reveal the dynamical effects at scales suggested by modeling of the few high-quality Chandra or XMM grating spectra. Greater sensitivity and resolving power will provide such data for more than the few dozen[22] stars accessible to today's observatories at high resolution. While the ÆGIS effective area will provide access to many more stellar systems, the new door opened will be on the kinematics of the high-energy emission at unprecedented levels. In fact, *ÆGIS will resolve the thermal line widths of coronal plasmas*.

TW Hya is the best-studied accreting Classical T Tauri system to date;[7,31] it serves as a prototype of a much larger class observable with ÆGIS, being the nearest, brightest of its class. TW Hya has very soft and metal-depleted X-ray emission which presumably comes from an accretion shock, funneled by magnetic fields (see Figure 8). A model-predicted post-shock downflow of $100\,\mathrm{km\,s^{-1}}$ has not yet been observed. With ÆGIS, we will centroid lines to $\sim 20\,\mathrm{km\,s^{-1}}$. Turbulent broadening may have been marginally detected by a deep Chandra grating spectrum[7], and would be clearly resolved by ÆGIS at $\sim 100\,\mathrm{km\,s^{-1}}$; the origin of UV and optical line broadening seen on this scale is not understood[23] and X-ray spectra would show whether the dynamics extend to higher temperature material. There are only about a dozen other accreting T Tauri systems bright enough for XMM to have *detected* excesses in O VII relative to O VIII emission (a proxy for accretion)[21], and only about 5 of these have definitive density measurements. ÆGIS can revolutionize stellar accretion disk studies by providing density and kinematic diagnostics for all these systems and many more.

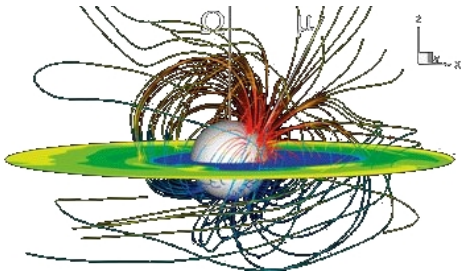

Figure 8: *ÆGIS spectra can resolve the inflow/outflow velocities of accretion streams and shocks as they are channeled by magnetic fields coupling the photosphere and accretion disk. (From Long, Romanova & Lovelace[40]).*

Other areas, currently poorly understood, will benefit from resolving bulk flows and more completely determine the kinetic energy budget; this falls under the NWNH category of rotation and magnetic field effects in stars (see Table 1). Some young stars have outflows in jets, driven by accretion, and harboring shocks in the outflows.[22] Optical studies show flows on the order of $200\,\mathrm{km\,s^{-1}}$, but there are no X-ray measurements. Solar flares have upflows and downflows of up to $200\,\mathrm{km\,s^{-1}}$, and accretion-driven upflows into coronal loops are expected to be of order $20\,\mathrm{km\,s^{-1}}$. These velocities would be easily determined by ÆGIS and help to characterize a stellar system's angular momentum, disk irradiation, and magnetic dynamo.

3 The ÆGIS Payload

3.1 ÆGIS Science Instruments

ÆGIS exploits modern mirror and grating technology to provide enormous gains in effective area and a critical improvement in resolving power (see Figure 2) at modest cost.

The major payload components are a Flight Mirror Assembly (FMA), a Grating Array Structure (GAS),and a Focal Plane Assembly (FPA). The FMA holds a Wolter-I optic comprised of concentric segmented slumped-glass mirrors. This optic, with a $4.4\,\mathrm{m}$ baseline focal length (much shorter than IXO's 20m) enables a grating spectrometer effective area comparable to IXO's at vastly lower cost. Mirror characteristics will be optimized in future design studies.

The GAS is mounted close to the FMA and holds six pairs of CAT grating arrays; the novel CAT gratings are described in detail below. The FPA consists of three CCD cameras to record dispersed spectra and a single CCD camera to provide 0^{th} order imaging. An Optical Bench Assembly maintains the mirror, gratings and detectors in the proper alignment. Each of the ÆGIS payload components has been studied in detail in the course of IXO definition studies. This gives us confidence in our estimates of the mass, power and bandwidth required, in the more compact, and much lower-cost configuration of ÆGIS.

ÆGIS instrumentation builds on strong heritage. The optical design is a direct design descendant of the high-resolution spectrographs built by the ÆGIS team and now flying on Chandra. The mirror technology was intensively developed for IXO and used to produce flight mirrors for NuSTAR, which will launch within the next few months. Grating fabrication builds on techniques developed for Chandra and benefits from substantial NASA facilities and technology development in the MIT Space Nanostructures Laboratory over the past decade. The focal plane MIT Lincoln Laboratory CCDs derive directly from devices now flying on Chandra and Suzaku,

3.2 Optical Design

ÆGIS has six independent objective CAT grating spec-

Parameter	Value	Units	Remarks
Spectrometer[1]			
Effective Area	1440	cm^2	@O VIII Lyα (0.653 keV)
	> 800	cm^2	$0.25 - 0.9$ keV
$E/\Delta E$	> 3500		$0.25 - 2$ keV
Mirror[1]			
Focal Length	4.4	m	
Diameter	1.9	m	
HPD (on-axis)	10	arcsec	
Mass	255	kg	
Power	175	W	heaters
CAT Gratings			
Blaze angle	3.5	deg	
Periods	200, 230	nm	arranged in opposing pairs
Mass	9.1	kg	
Power	0	W	
Focal Plane Assembly[1]			
Spec. Cameras	3		+ 1 0^{th} order
Arrays/Camera	2		
CCDs/Array	4		
CCD			
Type	BI		MIT/Lincoln
Size	25x25	mm	24μm pixel
Frame Rate	15	Hz	
Mass	60.4	kg	
Power	75	W	

Table 2: *Payload summary for baseline ÆGIS mission.*
[1] *Current best estimates for spectrometer performance, mass and power.*

trographs[28] that operate in parallel, with each served by a pair of diametrically opposed $\sim 30^\circ$ sectors (sub-apertures) of the FMA (see Fig 9). Dividing the telescope into 12 sub-apertures maximizes the spectral resolving power achievable from the ÆGIS mirror because each sub-aperture produces a Line-Spread Function (LSF) in the dispersion direction which is a factor of several smaller than the full-aperture point spread function. For ÆGIS a LSF with FWHM $\lesssim 3$" is sufficient to achieve $R > 3000$. This is obtained by sub-aperturing a mirror of 10" half-power diameter in the ÆGIS design. Each mirror sector is fitted with an array of light-weight blazed Critical-Angle Transmission (CAT) gratings.[26] Each grating array produces a separate dispersed spectrum. To maximize spectral resolution, the gratings for each sector are oriented to disperse normal to the local mirror radius (see Figure 9). The local dispersion direction is thus nearly normal to the dominant mirror scattering direction.

The gratings behind diametrically opposed sectors are blazed to share a single readout array, and the compact ÆGIS payload allows the six spectrographic readout arrays to be packaged in only three focal plane cameras. The gratings in diametrically opposed arrays have different periods (200 nm or 230 nm, respectively). This smoothes the effective area curve and provides additional wavelength redundancy in case of a single CCD failure. A CCD at the telescope focus provides 0^{th} order images with half power diameter on-axis of ~ 10 arcsec. Gratings and readouts for each spectrometer follow the surface of a Rowland torus, similar to the optical designs for the Chandra HETG[8] and XMM RGS.[15] Limiting the band to < 2 keV allows the use of larger graze angles, giving a lower mass and a more compact system.

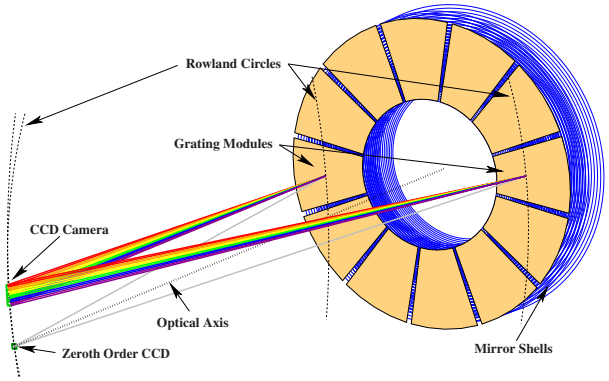

Figure 9: *Schematic of the dispersion geometry for a pair of CAT sectors, comprising one (out of six) CAT grating spectrometers. The mirrors are completely covered by 12 grating sectors.*

3.3 Flight Mirror Assembly

The large outer diameter and the need for sub-aperturing are well-matched to a segmented mirror design. The segmented glass mirror technology that has been under development for IXO and is being used on NuSTAR is ideally suited for this purpose.[60–62] The entire mirror assembly is segmented into two radial rings, the inner one covering radii from 460 mm to 650 mm and the outer one from 650 mm to 930 mm. The inner ring is further divided into 12 identical 30° modules in azimuth and the outer ring into 24 identical 15° modules. This makes the optics production amenable to parallel and mass production, reducing both schedule and cost. In addition, the small ($f/2.3$) focal ratio (relatively large graze angles) translates into a small number of mirror shells: 63, barely $1/6^{th}$ of IXO's 360. ÆGIS mirror sectors are made in a four-step process: (1) The 2×63 forming mandrels, which give the segments their figure, are fabricated. The same mandrels are used for all modules. (2) Mirror segments are made by slumping thin glass sheets on the mandrels and coating them to optimize X-ray reflectance; (3) Mirror segments are aligned and bonded into modules; and finally (4) Mirror modules are aligned and integrated into mirror sectors to which the grating arrays will be attached.

3.4 CAT Gratings

The recently developed CAT gratings combine the advantages of traditional transmission gratings (low mass, relaxed alignment and figure tolerances, transparency at higher energies) with those of blazed reflection gratings (high broad-band diffraction efficiency, higher dispersion, with its accompanying higher resolving power, at shorter wavelengths due to blazing into higher diffraction orders).

Low-mass, large area grating arrays are fixed in place immediately behind the mirrors to intercept and disperse the light reflected from them. By placing the gratings at maximum distance from the focus, the dispersion distance and resolving power are maximized. The CAT gratings are fabricated from silicon wafers using nano-fabrication techniques. They are described in more detail in a companion RFI response on grating technology.[25]

3.5 Focal Plane Assembly

The readout arrays incorporate detectors derived directly from those now flying on Chandra and Suzaku. Each is a 100 mm-long, linear array of 4 back-illuminated, frame-transfer CCD detectors. The high-quality backside passivation, as demonstrated on Suzaku, provides high quantum efficiency and excellent spectral resolution ($\Delta E = 50 - 80$ eV) to separate multiple spectral orders dispersed by the gratings. In operation the CCDs are passively cooled to 183 K. Two spectroscopic readout arrays are contained within each camera housing, and three such cameras are mounted in the focal plane. A fourth camera contains a single CCD to provide an accurate origin for the wavelength scales along with 10" (HPD) imaging on-axis and a 19' $\times$ 19' FOV (see Fig. 10). While (by design) the gratings diffract most E $<$ 1 keV photons to the spectroscopic readouts, higher energy photons are transmitted through the thin CAT gratings (only 6μm thick) to the $0^{\rm th}$ order image. The collecting area of the $0^{\rm th}$ order imager peaks above $1000\,{\rm cm}^2$ at 1.5 keV and exceeds $500\,{\rm cm}^2$ between 1.1 and 1.9 keV. The CCDs are read at a frame rate of 15 Hz. Each camera is served by a dedicated detector electronics assembly, and the entire focal plane is served by a single, internally redundant digital processing assembly.

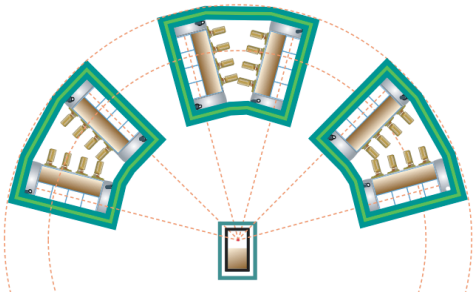

Figure 10: *Layout of the ÆGIS FPA, showing the 3 cameras with two readout arrays in each. Each CCD is* $(25\,{\rm mm})^2$ *in size with* 25 μm *pixels. The radius of the outer circle is* ~ 370 mm.

3.6 Technology Readiness & Development

ÆGIS technology readiness has advanced steadily in accordance with detailed plans. We briefly summarize technology readiness levels (TRL) and development plans for ÆGIS components here.

Mirror TRL: As of October 2011, we have successfully fabricated fused quartz mandrels and mirror segments that meet ÆGIS requirements. We have successfully and repeatedly aligned and bonded single pairs of mirror segments into module housing simulators and achieved X-ray images better than 10 arc-second HPD and LSF FWHM $<$ 3", meeting ÆGIS requirements (Figure 11).[17] We therefore judge the mirror to be at TRL 4 at present and expect TRL 5 by the end of CY2012. (See the companion RFI response by Zhang et al.)[59]

Figure 11: *(Left) Mirror segments have been aligned and bonded to a housing simulator. (Right) The image obtained from* 4.5 keV *Ti-K X-rays shows the effect of sub-aperturing—projection onto the x-axis yields 1.4" FWHM.*

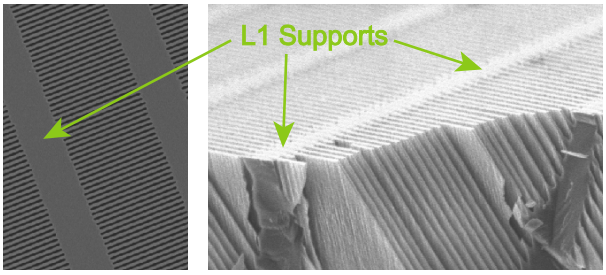

Figure 12: *Scanning electron micrograph of a dry-etched, free-standing* $25 \times 25\,{\rm mm}^2$ *grating membrane with* 200 nm *period Si CAT grating bars and an integrated "Level 1" support mesh. Left: Bottom view. Right: Cleaved cross section.*

Grating TRL: The required ultra-high aspect ratio grating bar geometry (150:1) has been successfully demonstrated. X-ray performance of small wet-etched prototypes is in good agreement with theory.[26]. The CAT technology was judged to be TRL 3 in 2009 when these milestones were reached. Since then, dry-etched, large-area ($\sim$ 6 cm^2), free-standing samples with the full hierarchy and complexity of support structures have been fabricated (see Fig. 12),[27] and we expect to achieve TRL 4 within a year.

FPA TRL: The ÆGIS FPA could be implemented with existing, flight-proven technology and meet all requirements except the 15 Hz readout rate. The CCDs now flying on Suzaku meet ÆGIS requirements for pixel-size, array size, detection efficiency and spectral resolution. The camera design is a simplified (and smaller) version of the ACIS camera now flying on Chandra. The detectors have

been judged TRL 5 (relative to the 15 Hz readout rate requirement) in IXO evaluations. The required readout rate has been demonstrated on several optical CCD devices and the required design modifications are summarized below.

Technology Development Plans: Detailed technology development plans for ÆGIS technology were defined in IXO studies. Here we summarize steps required to achieve TRL 5. With adequate funding we expect to be able to achieve all of these milestones in the next 2-3 years. **Mirrors:** 1) Implement alignment and bonding procedure for co-alignment and bonding of multiple pairs. 2) Verify long-term alignment stability of epoxy-bonded mirrors. 3) Construct and evaluate proto-type modules containing multiple pairs.
Gratings: 1) Minimize area of support structures that block X-rays. 2) Demonstrate KOH polishing and X-ray performance of dry-etched samples. 3) Integrate/align grating membrane and facet frame. 4) Demonstrate breadboard grating array. 5) Environmental tests.
FPA: 1) Implement CCD bus strapping and high responsivity output nodes on ÆGIS devices. 2) Demonstrate low-power analog processors.

4 The ÆGIS Mission

4.1 Mission Description

ÆGIS achieves its science objectives with a powerful payload in a mission of moderate size and cost. A capable but conventional spacecraft, an efficient orbit, and a modern operations model serve to maximize science return on investment. Key characteristics of the nominal ÆGIS mission adopted for costing purposes are presented in Table 3. We will refine these in future definition studies.

ÆGIS requirements are met by conventional spacecraft architectures and components. Figure 13 shows the baseline spacecraft concept in its launch configuration and as deployed. Aspect information is provided by a pair of star trackers on the bus and a fine guidance sensor mounted on the focal plane. Following the successful Swift approach, the attitude control system supports safe slewing in response to time/target-coordinate pairs in the command load. Onboard command and science data storage capacity permits autonomous operation for nearly 2 weeks without command or data loss, minimizing operations costs (see below). Note that science data downlink rates are quite modest thus are not a technology concern.

A number of launchers, including Falcon-9 and Atlas V-401, can place ÆGIS in the baseline halo orbit at Sun-Earth L2 with ample performance margin. The cost-effective Falcon-9 is baselined. The L2 orbit provides excellent observing efficiency and a stable thermal environment that simplifies payload and spacecraft design. The launch vehicle carries ÆGIS directly to L2; the spacecraft's onboard propulsion system provides orbital injection and subsequent station keeping. The nominal 3-year primary mission provides more than 70 Ms of science exposure time. This exceeds the time programmed for IXO XGS observations by a factor greater than 4. The environment at L2 and the requirements it places on the ÆGIS payload and spacecraft are well-understood from extensive IXO definition studies. These included exercises in the Instrument Design and Mission Design Laboratories at Goddard Space Flight Center.

Parameter	Value	Units	Remarks
Payload[1]			
Mass	325	kg	
Power	250	W	
Telemetry	128/1280	kbps	avg./peak
Spacecraft[1]			
Mass	385	kg	
Power	320	W	
Pointing control	30	arcsec	max. deviation (200 ks)
	1	arcsec s^{-1}	max. drift rate
Pointing knowledge	1.3	arcsec	3σ per axis
Observatory[2]			
Mass	1090	kg	at launch
Power			
Total	740	W	
Capability	1330	W	EOL
Margin	590	W	44% EOL
Telemetry	208	kpbs	average
Recorder	24	Gbyte	12.7 days
Mission			
Launcher			
Vehicle	Falcon-9		std. fairing
Capability	2010	kg	to L2
Margin	920	kg	46%
Orbit	L2		Sun-Earth
Duration			
Prime	3	yr	
Goal	5	yr	
Comm.	1	day^{-1}	DSN

Table 3: *Characteristics of a baseline ÆGIS mission which will be refined in future definition studies.*
[1] *Current best estimates shown for payload and spacecraft.*
[2] *Observatory parameter values include 30% contingency.*

An Earth-trailing drift-away orbit, like that used by Spitzer and Kepler, also appears to be a viable option, as it can be reached with the same launchers and would provide essentially the same observing efficiency. We will evaluate the tradeoffs between these candidate orbits in future defintion studies.

ÆGIS will be open to all astronomers with peer-reviewed competition for all observing time after allowances for a short initial verification period and a small ($\sim$ 5%) allocation for calibration and engineering purposes. ÆGIS will minimize mission planning costs by using month-long planning cycles. Daily communications with the spacecraft are envisioned, mostly for purposes of monitoring health and safety, although as noted above the spacecraft would be capable of autonomous operation for nearly two weeks. Command load segments could be

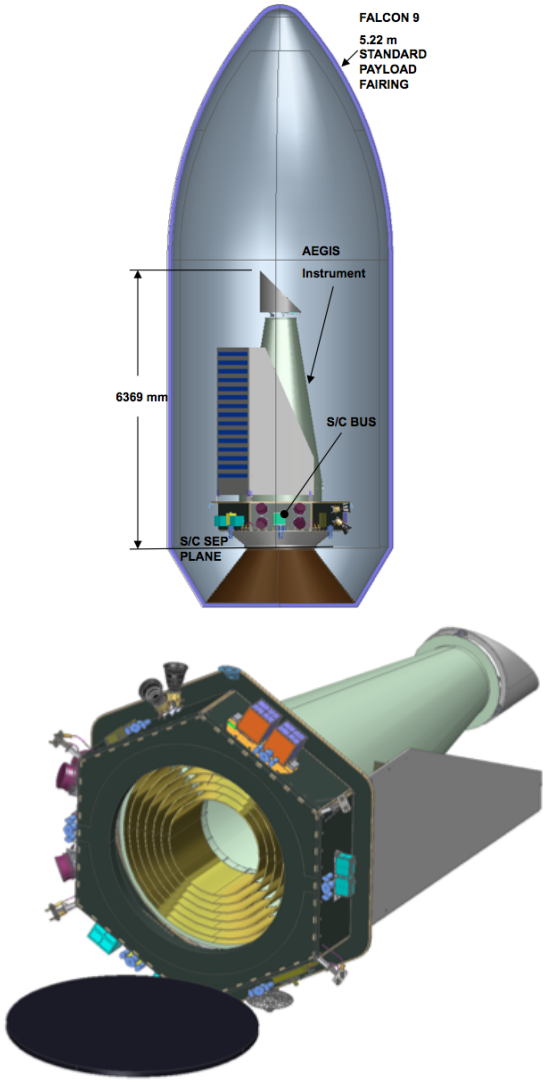

Figure 13: *ÆGIS in Falcon-9 standard fairing (top) and as deployed (bottom). Graphics produced by Ball Aerospace.*

updated and data downloaded in those communications. Target-of-Opportunity (TOO) observations could be accommodated without significant impact to the monthly plan since the L2 orbit is relatively free from complications such as momentum build-up, radiation belt passages, and eclipse management which drive Chandra and XMM-Newton mission planning.

4.2 Cost and Basis of Estimate

The ÆGIS ROM estimated total mission cost of $758M in FY2012 dollars, including launch services and reserves, is near the low-end of the medium-cost category. ROM cost estimates for major elements of the baseline ÆGIS mission are presented in Table 4. Spacecraft, management, systems engineering, mission assurance, and integration and test cost estimates are based on advice from experienced contractors and are consistent with commonly accepted scaling rules. Mirror and instrument costs were obtained by scaling detailed PRICE-H estimates developed during IXO definition studies, incorporating grass-roots estimates for grating element and CCD detector costs developed at MIT. Payload costs include 6-months of mirror and instrument calibration at Marshall Space Flight Center's X-ray and Cryogenic Facility (XRCF). Launch cost is estimated from public commercial sources, confirmed by contractors, and includes an allocation for NASA oversight.

Flight operations costs appropriate for a probe-class mission are based on industry estimates of 15 FTEs including cross-trained engineers, controllers and planners with managerial and administrative support. Cost for an observatory-class mission would be slightly higher. Pre-launch operations costs include all elements required to prepare for full operations support at launch, including all modifications to the Chandra data system required to produce archival quality data products. DSN communications costs include early flight operations followed by a single 30 minute contact per day. Science operations costs capture calibration, operations, planning and administrative functions as well as peer review and grants administration. The observer grants budget would support, for example, 200 programs per year averaging 125ks at $50k (FY2012), together with a small number of postdoctoral fellows. A theory program during the early mission would transistion to an archival program later in the mission.

Mission Element	**ROM Cost (M$, FY2012)**	**Remarks**
Management, Sys. Engineering, & SMA	68	
Payload		
Mirror	130	GSFC
GAS & FPA	93	Price-H & MIT
Calibration	3	MSFC XRCF
Observatory		Contractor est.
Spacecraft	112	
I & T	16.4	
Launch support	7.8	incl. pre-launch
Launch Services	75	Falcon-9 with oversight
Operations		3 years
Pre-launch	28	Flt. & Sci.
Flight & Comm.	16	DSN, 3 years
Science	25.5	
Observers	40	GO program
CBE Total	615	
Reserves[1]	143	
MISSION TOTAL	**758**	

Table 4: *ÆGIS misson cost is in the medium-cost category.*
[1] *Reserves: 30% in Phases A-D excluding launch; 20% in Phase E excluding GO program.*

Acknowledgements

The ÆGIS science team is grateful for technical support and advice from a group at Ball Aerospace and Technologies Corporation, led by Steve Jordan; from a group at Lockheed Martin Corporation, led by Domenick Tenerelli; and from Chuck Lillie and Suzi Casement at Northrup Grumman Aerospace Systems.

References

[1] Armitage, P. J., 2011, ARA&A, 49, 195

[2] Blustin, A. J., et al., 2005, A&A, 431, 111

[3] Bookbinder, J., 2010a, ArXiv e-prints, 1001.2329

[4] Bookbinder, J., 2010b, ArXiv e-prints, 1003.2847

[5] Bregman, J. N., & Lloyd-Davies, E. J., 2007, ApJ, 669, 990

[6] Bregman, J. N., et al., 2009, ApJ, 699, 1765

[7] Brickhouse, N. S., et al., 2010, ApJ, 710, 1835

[8] Canizares, C. R., et al., 2005, PASP, 117, 1144

[9] Cen, R., & Fang, T., 2006, ApJ, 650, 573

[10] Cen, R., & Ostriker, J. P., 2006, ApJ, 650, 560

[11] Committee for a Decadal Survey of Astronomy and Astrophysics, (eds.) 2010, "New Worlds, New Horizons in Astronomy and Astrophysics", The National Academic Press, Washington, DC (NWNH)

[12] Crenshaw, D. M., et al., 1999, ApJ, 516, 750

[13] Danforth, C. W., & Shull, J. M., 2008, ApJ, 679, 194

[14] Danforth, C. W., Stocke, J. T., & Shull, J. M., 2010, ApJ, 710, 613

[15] den Herder, J. W., et al., 2001, A&A, 365, L7

[16] Evans, D. A., et al., 2010, in X-ray Astronomy 2009: Present Status Multi-wavelength Approach and Future Perspectives, Vol. 1248, 425

[17] Evans, T., et al., 2011, 8147, 81470P

[18] Fabian, A. C., et al., 2009, Nature, 459, 540

[19] Fukugita, M., & Kawasaki, M., 2003, MNRAS, 343, L25

[20] Glassgold, A. E., Feigelson, E. D., & Montmerle, T., 2000, Protostars and Planets IV, 429–+

[21] Güdel, M., & Telleschi, A., 2007, A&A, 474, L25

[22] Güdel, M., et al., 2007, A&A, 468, 515

[23] Günther, H. M., & Schmitt, J. H. M. M., 2008, A&A, 481, 735

[24] Hanke, M., et al., 2009, ApJ, 690, 330

[25] Heilmann, R., et al., 2011, Critical-Angle Transmission Gratings for High-Resolution Soft X-Ray Spectroscopy, RFI/NNH11ZDA018L: Mission Concepts for X-ray Astronomy, NASA)

[26] Heilmann, R. K., et al., 2011a, Appl. Opt., 50, 1364

[27] Heilmann, R. K., et al., 2011b, in Optics for EUV, X-Ray and Gamma-Ray Astronomy V, ed. S. L. O'Dell, G. Pareschi, Vol. 8147, 81471L

[28] Heilmann, R. K., et al., 2010, in Space Telescopes and Instrumentation 2010: Ultraviolet to Gamma Ray, ed. M. Arnaud, S. S. Murray, T. Takahashi, Vol. 7732, 77321J

[29] Hoekstra, H., et al., 2005, ApJ, 635, 73

[30] Kaspi, S., et al., 2002, ApJ, 574, 643

[31] Kastner, J. H., et al., 2002, ApJ, 567, 434

[32] Krongold, Y., et al., 2007, ApJ, 659, 1022

[33] Lee, J. C., 2010, Space Sci. Rev., 157, 93

[34] Lee, J. C., et al., 2009a, in astro2010: The Astronomy and Astrophysics Decadal Survey, Vol. 2010, 178

[35] Lee, J. C., et al., 2009b, ApJ, 702, 970

[36] Liang, G. Y., & Zhao, G., 2008, AJ, 135, 2291

[37] Liu, J., Mao, S., & Wang, Q. D., 2011, MNRAS, 415, L64

[38] Liu, J., et al., 2010, MNRAS, 404, 1879

[39] Loewenstein, M., & Davis, D. S., 2010, ApJ, 716, 384

[40] Long, M., Romanova, M. M., & Lovelace, R. V. E., 2008, MNRAS, 386, 1274

[41] Miller, J. M., et al., 2011, ApJ, 731, L7+

[42] Miller, J. M., et al., 2006, Nature, 441, 953
[43] Miller, J. M., et al., 2008, ApJ, 680, 1359
[44] Nardini, E., et al., 2011, MNRAS, 410, 1251
[45] Nicastro, F., Fiore, F., & Matt, G., 1999, ApJ, 517, 108
[46] Nicastro, F., et al., 2005, ApJ, 629, 700
[47] Nicastro, F., et al., 2003, Nature, 421, 719
[48] Ogle, P. M., et al., 2004, ApJ, 606, 151
[49] Petric, A., et al., 2006, ApJ, 651, 41
[50] Pipino, A., & Matteucci, F., 2011, A&A, 530, A98+
[51] Reynolds, C. S., 1997, MNRAS, 286, 513
[52] Reynolds, C. S., et al., 1995, MNRAS, 277, 901
[53] Schröter, S., et al., 2011, A&A, 532, A3+
[54] Stella, L., 1990, Nature, 344, 747
[55] Turriziani, S., Cavazzuti, E., & Giommi, P., 2007, A&A, 472, 699
[56] Werner, N., et al., 2009, MNRAS, 398, 23
[57] Williams, R. J., Mathur, S., & Nicastro, F., 2006, ApJ, 645, 179
[58] Yao, Y., et al., 2009, ApJ, 697, 1784
[59] Zhang, W., 2011, Next Generation X-ray Optics: High-resolution, Lightweight, and Low-cost, RFI/NNH11ZDA018L: Mission Concepts for X-ray Astronomy, NASA)
[60] Zhang, W. W., et al., 2009, 7437, 74370Q
[61] Zhang, W. W., et al., 2010, 7732, 77321G
[62] Zhang, W. W., et al., 2011, 8147, 81470K

A ÆGIS Team

G. E. Allen	MIT	gea@space.mit.edu
M. W. Bautz	MIT	mwb@space.mit.edu
J. Bookbinder	SAO	jbookbinder@cfa.harvard.edu
D. Bower	Lockheed Martin Co.	daniel.r.bower@lmco.com
J. Bregman	University of Michigan	jbregman@umich.edu
N. Brickhouse	SAO	bhouse@head.cfa.harvard.edu
D. N. Burrows	Pennsylvania State University	burrows@astro.psu.edu
C. R. Canizares	MIT	crc@space.mit.edu
S. Casement	NGAS	suzanne.casement@ngc.com
D. Chakrabarty	MIT	deepto@space.mit.edu
K.-W. Chan	NASA/GSFC	kai-wing.chan-1@nasa.gov
B. Costello	Lockheed Martin Co.	bill.costello@lmco.com
J. E. Davis	MIT	davis@space.mit.edu
D. Dewey	MIT	dd@space.mit.edu
J. J. Drake	CfA	jdrake@head.cfa.harvard.edu
M. S. Elvis	SAO	elvis@cfa.harvard.edu
D. Evans	Elon University/CfA	devans@cfa.harvard.edu
A. Falcone	Pennsylvania State University	afalcone@astro.psu.edu
K. Flanagan	STScI	flanagan@stsci.edu
R. Heilmann	MIT	ralf@space.mit.edu
J. C. Houck	MIT	houck@space.mit.edu
D. P. Huenemoerder	MIT	dph@space.mit.edu
S. Jordan	Ball Aerospace	sjordan@ball.com
A. Klavins	Lockheed Martin Co.	aklavins@msn.com
J. C. Lee	Harvard University	jclee@cfa.harvard.edu
J. Lempke	Lockheed Martin Co.	jim.lempke@lmco.com
C. Lillie	NGAS	chuck.lillie@ngc.com
M. Loewenstein	NASA/GSFC	michael.loewenstein-1@nasa.gov
H. L. Marshall	MIT	hermanm@space.mit.edu
S. Mathur	Ohio State University	smita@astronomy.ohio-state.edu
R. S. McClelland	SGT	ryan.s.mcclelland@nasa.gov
J. M. Miller	University of Michigan	jonmm@umich.edu
R. Mushotzky	University of Maryland	richard@astro.umd.edu
T. Nguyen	Lockheed Martin Co.	thang.nguyen@lmco.com
F. Nicastro	SAO	fabrizio.nicastro@oa-roma.inaf.it
M. A. Nowak	MIT	mnowak@space.mit.edu
S. L. O'Dell	NASA/MSFC	steve.o'dell@nasa.gov
F. Paerels	Columbia University	frits@astro.columbia.edu
R. Petre	NASA/GSFC	robert.petre-1@nasa.gov
A. Ptak	NASA/GSFC	andrew.f.ptak@nasa.gov
T. T. Saha	NASA/GSFC	timo.t.saha@nasa.gov
M. Schattenburg	MIT	marks@space.mit.edu
N. Schulz	MIT	nss@space.mit.edu
R. K. Smith	SAO	rsmith@cfa.harvard.edu
D. Tenerelli	Lockheed Martin Co.	domenick.tenerelli@lmco.com
R. Vanbezooijen	Lockheed Martin Co.	roel.vanbezooijen@lmco.com
G. Vasudevan	Lockheed Martin Co.	gopal.vasudevan@lmco.com
D. Wang	University of Massachusetts, Amherst	wqd@astro.umass.edu
S. Wolk	CfA	swolk@cfa.harvard.edu
W. W. Zhang	NASA/GSFC	william.w.zhang@nasa.gov

B Acronym List

ACIS	Advanced CCD Imaging Spectrometer
AEGIS	Astrophysics Experiment for Grating and Imaging Spectroscopy
AGN	Active Galactic Nucleus
CAT	Critical Angle Transmission
CBE	Current Best Estimate
CCD	Charge Coupled Device
COS	Cosmic Origins Spectrograph
DSN	Deep Space Network
EOL	End of Lifetime
ESA	European Space Agency
EW	Equivalent Width
FMA	Flight Mirror Assembly
FOV	Field of View
FPA	Focal Plane Assembly
FWHM	Full Width Half Maximum
GAS	Grating Array Structure
GO	Guest Observer
HEG	High Energy Grating
HETG	High Energy Transmission Grating
HETGS	High Energy Transmission Grating Spectrometer
HPD	Half Power Diameter
HST	Hubble Space Telescope
IGM	Intergalactic Medium
ISM	Interstellar Medium
IXO	International X-ray Observatory
LETG	Low Energy Transmission Grating
LMC	Large Magellanic Cloud
LSF	Line Spread Function
MEG	Medium Energy Grating
NS	Neutron Star
NWNH	“New Worlds, New Horizons” (a.k.a., “Decadal Survey 2010”)
OBF	Optical Blocking Filter
PMS	Pre-Main-Sequence
RFI	Request for Informtion
RGS	Reflection Grating Spectrometer
ROM	Rough Order of Magnitude
SAT	Strategic Astrophysics Technology
SMA	Safety and Mission Assurance
SMBH	Super-massive Black Hole
SMC	Small Magellanic Cloud
SXS	Soft X-ray Spectrometer
TOO	Target of Opportunity
TRL	Technical Readiness Level
WHIM	Warm-Hot Intergalactic Medium
XGS	X-ray Grating Spectrometer
XIS	X-ray Imaging Spectrometer
XMM	X-ray Monitoring Mission
XRB	X-ray Binary